Macroparticle Traffic Simulation Model To Investigate Peak-Period Commuter Decision Dynamics

GANG-LEN CHANG, HANI S. MAHMASSANI, and ROBERT HERMAN

ABSTRACT

A special-purpose, macroscopic highway corridor traffic simulation model is presented. The model views traffic as discrete vehicle bunches or macroparticles that are moved according to local speeds defined by local concentrations, resulting in high computational efficiency. The model allows the investigation of commuter decision dynamics and their interrelation with time-dependent congestion patterns. Two applications of the model are described illustrating its use (a) in conjunction with behavioral rules by which commuters respond to experienced congestion and (b) as part of an interactive experiment involving decision making by real commuters.

Peak-period traffic congestion is an everyday occurrence in most metropolitan areas, particularly in commuting corridors. The excessive delay, instability of travel time, and increased fuel consumption that accompany congestion translate into significant economic and social cost. With the well-known difficulties that preclude the expansion of roadway capacity in urban areas, most efforts to relieve congestion during the past decade have centered on improving system usage through traffic control as well as demand-side strategies. An understanding of the day-to-day interaction between traffic patterns and commuters' departure time and route choice behavior is essential to the analysis of peak-period congestion and the design and proper evaluation of control measures.

Some recent analytical studies have addressed commuter departure time decisions and the resulting temporal traffic pattern in a dynamic user equilibrium framework (1-5). Most of these studies have considered an idealized system with a single origin and a single destination, with congestion occurring at a unique bottleneck along the only available route. However, a more realistic though more complex situation is that of multiple origins and multiple destinations in a particular commuting corridor, where congestion may develop at more than one location and vary from day to day.

The analysis of the interrelationship between the time-dependent congestion patterns and commuters' responses in such a system is actually too difficult to be tackled analytically under realistic assumptions. A more convenient and effective approach is to use a special-purpose simulation tool that can capture the complex dynamics of the system, particularly the fluctuation of travel time with departure time and the time-dependent congestion patterns. This tool should also possess the capability to explore the impact of control strategies of alternative user decision rules on the performance of the system and its convergence properties. It was in response to these needs that the Macroparticle Simulation Model (MPSM) was developed.

The purpose of this paper is to introduce the logic employed in this special-purpose simulation model and to describe its application to ongoing research on the dynamics of user decisions and peak-period congestion. Further, because appropriate data for the study of commuters' departure time choice dynamics are quite difficult to obtain in a real-world context, interactive use of this program, in conjunction with survey techniques to study these phenomena, is discussed.

The general structure of this model and some of its key features are outlined in the next section, including a discussion of the inputs and major options available to the model user. In the second section computational experience and a brief sensitivity analysis with respect to key control variables are presented. The application of this model is the principal concern in the third section, in which is presented a summary of a number of computer simulation experiments that were conducted to investigate a commuting corridor system's convergence status under prespecified user decision rules. Further illustration of the model's application is given in the fourth section, in which a description is given of the use of the MPSM in conjunction with an interactive experimental procedure in which participants make daily departure time decisions in a hypothetical commuting situation. The variation of congestion patterns as well as the evolution of system concentration predicted by the MPSM, given the participants' choices, are examined therein. Finally, concluding comments and possible further extensions of this work are presented in the last section.

DESCRIPTION OF THE MPSM

Overview

Because the major concern is with the dynamics and convergence properties of the corridor system, the simulation program must possess the capability of providing the following information: (a) the concentration fluctuation in each section along the highway corridor for a given time-dependent demand, (b) the variation of travel time versus departure time for a given origin-destination pattern, and (c) the day-to-day evolution of the system's performance under various postulated rules that might govern users' departure time choice behavior.

Most of the existing macroscopic corridor simulation packages, such as MACK and SCOT, can meet these requirements (6,7). However, each simulation package was developed for applications that are not necessarily consistent with the present purpose, result-

ing in excess requirements and processing information and additional computational cost. These are important considerations in this research because the search for system covergence typically requires a considerable number of repeated simulations, often in excess of 50 simulation days. These considerations have led to the development of the special-purpose MPSM.

The MPSM is a fixed-time macroscopic traffic simulation model, which uses established traffic flow relationships to simulate the movement and the interaction of vehicles in a commuting highway corridor. Unlike most macroscopic simulation programs, for instance the MACK or FREFLO family (6,7), the traffic flow in the highway is not modeled as a compressible fluid but is viewed as a collection of vehicle groups or bunches, termed macroparticles [somewhat similar to the platoons used in the DAFT model (8,9)]. The model keeps track of the physical position of those particles using a prespecified speed-density relationship. The macroparticle approach avoids the significant computational cost of tracing individual vehicles, which is not essential to the present research. In addition, it avoids approximating traffic as a continuous fluid and the resulting inaccuracies such as the occurrence of nonphysical speeds. Further details regarding the tracing of vehicle movement are presented later in this section.

The MPSM consists of two principal components. The first component, or vehicle generation component, processes the daily decisions of users into sector-specific discretized time-dependent vehicle demand patterns. A user-decisions subroutine is also included to allow the researcher to specify departure time readjustment rules governing the behavior of commuters on a daily basis. The second component, or simulator, actually simulates the flow of traffic, including queueing at entrance ramps and vehicle movement along the highway. The overall framework and the interrelationship between each principal component are shown in Figure 1.

The input to the MPSM consists of two principal categories: supply-side data and demand-side information. The first category contains information on the key physical and operational features of the highway facility, such as the total corridor length, the number of analysis sections that the corridor is subdivided into, and the number of lanes as well as the allowable free flow speed in each section. The parameters of the speed-density model, as well as various simulation control parameters (described later in this section), are also included in this category.

The second category consists of information about usage level and commuter behavior. These are discussed hereafter in conjunction with the vehicle generation component of the model.

Vehicle Generation Component

The key demand-side input to the traffic simulation is the time-dependent vehicle departure patterns from each of the residential or origin sectors considered in the analysis. There are two principal approaches available to the model user; the approach used depends on the particular research application. The first approach consists of specifying the generation functions directly for a particular simulation day.

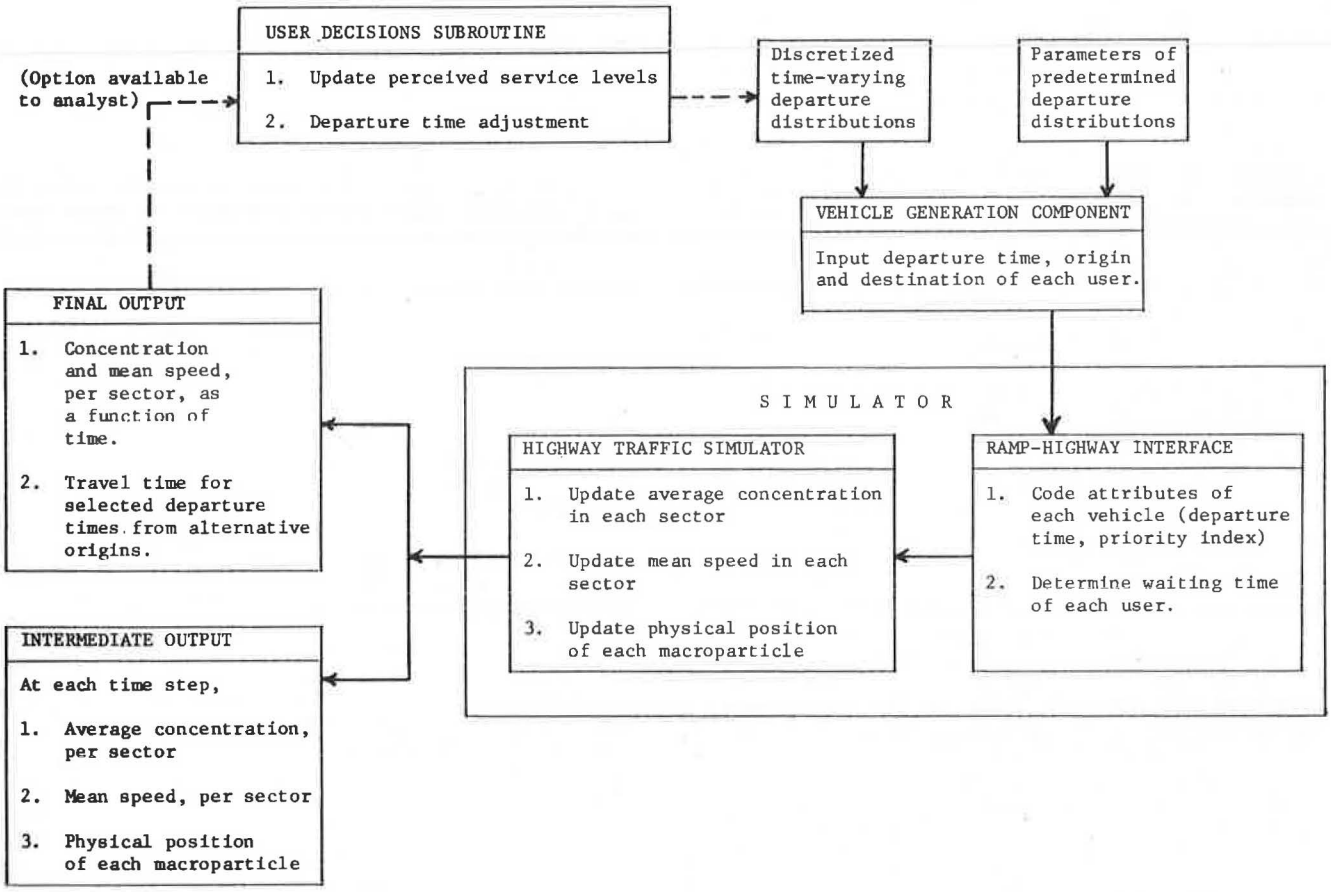

FIGURE 1 Overall framework of the MPSM.

The second approach treats the formation of the time-varying departure pattern endogenously, using individual decision rules to determine users' departure time choices on a given simulation day in response to the service levels experienced on previous days, as determined by the traffic simulation. This second approach would be appropriate when the objective is to investigate the effect of alternative models of individual behavior, or when such models have been calibrated on actual observations and are used to evaluate the effect of alternative control strategies on peak-period congestion.

When following the first approach, the model user can specify the departure time distributions in one of two forms: (a) as a discretized function giving the number of departures, from a particular origin, in each time interval or (b) as one of a number of commonly used distributions for which the model user has to supply the appropriate parameter values. An example application using this first approach will be given in the fourth section, where departure time decisions are made by real commuters participating in an interactive experiment. The vehicle generation component then processes the individual decisions into the desired time-dependent input functions.

Under the second approach, a user-decisions subroutine needs to be specified. It essentially takes the output of the traffic simulation on a given day, particularly travel time and schedule delay (defined as the difference between a commuter's desired arrival time and actual arrival time at the work destination), and determines each user's response in the form of a departure time selection for the following day. The rules used for this readjustment process constitute one important area of the overall research effort. Possible behavioral rules include those based on the widely used utility maximization principle (1,5), as well as other less restrictive heuristic rules reflecting so-called boundedly rational or "satisficing" behavior (10). A brief example application of this approach is given in the third section; further details of this particular aspect are outside the scope of this paper and can be found elsewhere (10).

Essentially, under the second approach, the simulations automatically proceed from one day to the next, as the individual decisions determined in the user-decision subroutine are internally transformed into time-dependent departure patterns. The process takes place over a prespecified maximum number of days or until steady state is reached, whichever occurs first. It should also be noted that, under either approach, additional demand-side input information includes users' respective desired arrival times (used in the schedule delay calculations), which need not necessarily be identical to their work start times, as well as the desired destination.

SIMULATOR

Ramp-Highway Interface

Every departing vehicle is assumed to start directly at the corresponding entry ramp onto the highway facility. Therefore access time from a specific residence to the ramp is not explicitly considered in these analyses, which is equivalent to implicitly assuming that it is a constant term and thus would merely shift a user's departure time by a fixed amount. A departing vehicle is identified by its departure time and the required travel distance (based on the desired destination). Naturally, vehicles cannot all enter the facility simultaneously due to physical and operational capacity constraints (including possible traffic control devices). Because the microscopic details of merging maneuvers are beyond the level of detail of the model, a simple deterministic queueing approximation is employed to handle this phenomenon.

Denoting the service rate by s, the queue length at time t by D(t), and the fixed simulation time step by Δt, a user wishing to depart in the interval $[t, t + \Delta t]$ is considered to incur a wait time only if $D(t) > s\Delta t$.

Note that the service discipline at the ramp queue is first come, first served. However, in the event that some users wish to depart simultaneously, the departures need to be ordered. A priority index is defined for this purpose and can be either assigned exogenously by the model user or randomly generated by the model using the Monte Carlo technique.

Vehicles leaving the queue are subsequently grouped in macroparticles for moving on the highway proper. When using a fixed macroparticle size, a minor problem arises when the number of entering vehicles does not form an integer number of complete macroparticles, thus delaying some vehicles until a sufficient number are present to complete that last group. Because a typical macroparticle size is between 5 and 10 vehicles, the resulting delay is often negligible and not in excess of Δt (Δt = 1 min was used in most of the simulations), except possibly at extremely low usage levels (when congestion is not of concern anyway). One way to get around this issue altogether is to use variable size macroparticles; in this case it is, however, recommended not to go below 5 vehicles per particle in order to maintain the computational cost advantages. Issues relating to macroparticle size are discussed hereafter in conjunction with traffic movement on the highway proper.

Highway Traffic Simulator

The highway traffic movement simulator is the core of the MPSM. This part of the program executes a set of procedures at every simulation interval, the length of which is user controlled and possibly different from that of the vehicle generation component. These procedures are described here and contrasted with other available models.

Most of the commonly used macroscopic simulation models (6,7,11,12), though developed for their own particular purposes, share the following set of assumptions: (a) time is discretized into small, equal intervals; (b) the highway facility is divided into sections; (c) traffic demand and system performance are effectively constant over a given time interval; and (d) traffic flow is viewed as a compressible fluid where the details of individual vehicle movement are inconsequential. Three basic equations are then used to govern the flow of traffic in the facility (12): a conservation equation, a speed-concentration relation, and the identity of flow to the product of speed and concentration. The conservation of vehicles can be stated as

$$k_i^{t+1} = k_i^t + [\Delta t/(\ell_i\ \Delta X_i)]\left[\ell_{i-1}\ q_i^{t+1} - \ell_i\ q_{i+1}^{t+1} + (N_i^{t+1}/\Delta t)\right] \quad (1)$$

where

k_i^t = concentration in section i during the t-th time step, in vehicles per lane-mile;

q_i^t = flow into section i during the t-th time step;
N_i^t = number of vehicles generated in section i minus those exiting in section i during the t-th time step;
ℓ_i = number of lanes of section i;
ΔX_i = length of section i; and
Δt = simulation time step.

The second equation is the speed-concentration relationship, which varies between the various models, and the third equation simply states that

$$q_i^{t+1} = k_i^t \, v_i^t \tag{2}$$

In the MPSM, both conservation and speed-concentration equations are used. However, as noted earlier, the flow relation (Equation 2) is not used. Instead, vehicles in the flow are viewed as groups of physical entities, termed macroparticles, and move in accordance with the local speed field, specified by a speed-concentration relation. Thus, the concentration of each section can be updated at every time step by tracing the actual physical positions of the particles. The general approach of tracing the position of groups of vehicles seems to have been adopted by the DAFT/SCOT family of simulation packages (8,9), in which vehicles are moved in platoons whose lengths are followed. In the MPSM, however, the length of the macroparticle need not be explicitly considered, as long as its size is not excessively large. The logic of the macroparticle approach adapted in this work follows that of the "magnetohydrodynamic particle code" developed for the fluid simulation of plasmas (13).

The conservation equation used in the MPSM then has the following form:

$$k_i^{t+1} = k_i^t + (1/\ell_i \, \Delta X_i) \left(M_i^{e,t+1} - M_i^{o,t+1} + N_i^{t+1} \right) \tag{3}$$

where $M_i^{e,t+1}$ and $M_i^{o,t+1}$ denote the vehicles that enter section i from the preceding section and those that move onto the next section, respectively, in a given time step Δt.

In the MPSM, the concentration in each section is updated, using Equation 3, at the beginning of every time step, and it is assumed to remain constant over the interval [t, t + Δt]. The corresponding mean speed prevailing during this interval can then be obtained from the speed-concentration relation. The functional form adopted in most of the simulations is

$$v_i^t = (v_f - v_0) \, (1 - k_i^t/k_0)^{\alpha} + v_0 \tag{4}$$

where

v_i^t = mean speed in section i during the t-th time step;
v_f, v_0 = mean free speed and minimum speeds on the facility, respectively;
k_0 = maximum or jam concentration; and
α = a parameter.

Note that the speed-concentration relation could be modeled using different or more elaborate formulations. However, this particular aspect has not been the focus of the present research, and Equation 4 has been found perfectly adequate to capture the character of the system's performance in the context of investigating the dynamic interaction between commuters' decisions and peak-period congestion.

Macroparticles are moved at the prevailing section mean speed, yielding the respective distances traveled during a particular time step and the resulting positions at the end of the interval. Section concentrations are subsequently updated, as described earlier, for the next time interval. In addition to its computational efficiency, tracing the macroparticles obviates the need for monitoring the traffic flow with a macroscopic flow equation (Equation 2). As mentioned earlier, the use of such a flow equation to control the flow from one finite section to another can transport material in unrealistically short times over long distances, thereby resulting in nonphysical high transport speeds. For example, if there are n finite sections in a linear highway, material will be transported every time interval Δt, no matter how small, so that some material will traverse n sections of finite length n $\cdot$ ΔX in the time nΔt, yielding the possibly unrealistic speed $\Delta X/\Delta t$, regardless of prevailing conditions. Further details on the particle-moving process are given hereafter.

Vehicle-Moving Process

The physical position of each macroparticle is updated at the end of every simulation interval and stored as one of the attributes of that macroparticle. Let X(i,m,t) denote the position of macroparticle m in section i (measured, in the direction of flow, relative to the beginning of the section) at the end of interval t, and R(i,m,t) the distance from its current position to the beginning of the next (downstream) section, as shown in Figure 2. Of course, R(i,m,t) = ΔX_i - X(i,m,t). The new position of particle m at the end of interval t+1 will be obtained by advancing it by a distance d(m,t+1) = $\Delta t \cdot v_i^{t+1}$ as long as d(m,t+1) $\leq$ R(i,m,t), meaning that its new position remains in section i.

In the event that d(m,t+1) > R(i,m,t), the particle will have to travel in the next section, i+1, during a fraction of the interval Δt. However, the mean speed in section i+1 may be different from that in the preceding section. The travel distance of macroparticle m during this Δt can thus be broken into two parts. The first part, which is equal to R(i,m,t), proceeds at the mean speed, v_i^{t+1}, for a fraction of the Δt equal to $R(i,m,t)/v_i^{t+1}$. In the remaining part of the time interval, namely $\Delta t' = \Delta t - [R(i,m,t)/v_i^{t+1}]$, travel takes place in section i + 1. Denote this second part of the distance traveled by R'(i+1, m,t+1). However, it does not seem reasonable to maintain a speed of v_i^{t+1}, nor to drastically change, midway, to v_{i+1}^{t+1}. A plausible way to handle this aspect is to assume that drivers will readjust their travel speed while entering i + 1 in a manner that is consistent with prevailing traffic conditions; the following averaging mechanism has been adopted in the model:

$$R'(i+1,m,t+1) = \Delta t' \left[(1/2) \left(v_i^{t+1} + v_{i+1}^{t+1} \right) \right] \tag{5}$$

Of course, the significance of this problem depends greatly on the size of the time step Δt, as well as on the section lengths. For sufficiently small Δt, the correction should not be of concern,

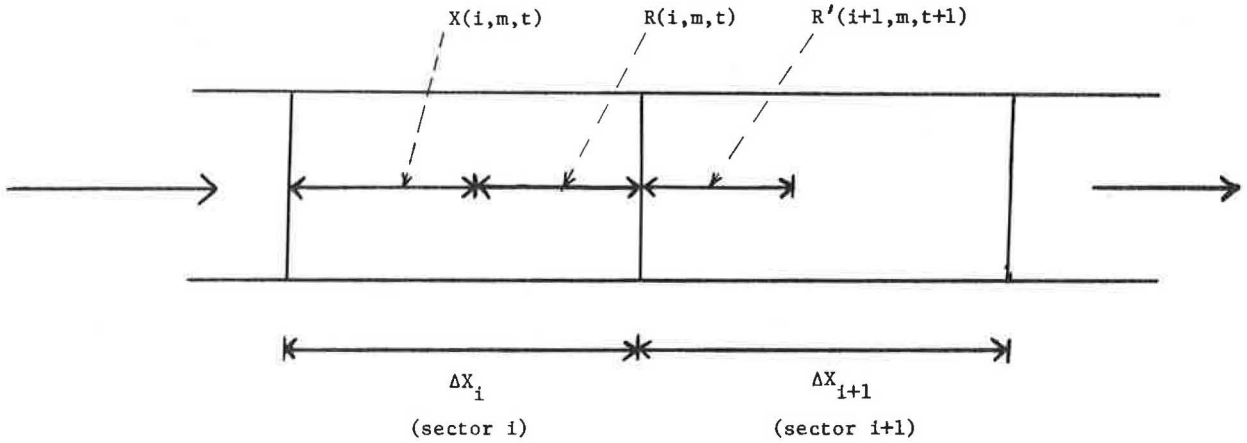

FIGURE 2 Graphic illustration of vehicle-moving process.

particularly for the present research applications. Selection of the number and lengths of the sections, of the time step Δt, and of the macroparticle size should be made judiciously. The frequently encountered trade-off between accuracy and computational efficiency is naturally present here. Sensitivity analyses have been conducted to provide useful insights into this aspect, as described in the next section.

MODEL USE CONSIDERATIONS AND SENSITIVITY ANALYSIS

In this section, some general considerations for selecting the key simulation parameters of the MPSM are discussed. In addition, the results of a number of numerical experiments conducted on the CDC system (Dual cyber 170/750) of the University of Texas at Austin are presented in order to better understand the effects of each key parameter. The numerical tests reported hereafter were carried out using a hypothetical 7-mile commuting corridor, with 2,400 trip makers uniformly distributed along its entire length, except for the last 1-mile section that immediately precedes the presumed common destination [central business district (CBD)]. In all cases, unless otherwise indicated, the highway facility was divided into seven 1-mile sections, with two lanes in each direction, though only the inbound (home-to-work) direction was considered here. The parameter values used in Equation 4 were $v = 45$ mph, $v_0 = 6$ mph, $k_j = 180$ vehicles per lane-mile, and $\alpha = 3.1416$ (or π).

There are three key simulation parameters in the MPSM: the simulation time step Δt, the macroparticle size Δm, and the section length ΔX. These are discussed in turn hereafter.

Selection of Section Length ΔX

As noted earlier, the continuous highway facility is usually divided into several discrete sectors in most macroscopic simulation models. Because system performance characteristics, such as concentration and speed, along each section are assumed to remain constant within each simulation time interval, a shorter section length can better reflect the location-dependent performance variation. Although the computational cost of course increases with the number of sectors specified (for a given total highway length), the relatively high efficiency of the MPSM is such that the incremental cost of increasing the number of sectors, or conversely of reducing ΔX, is rather small. This can be seen in Table 1 that gives the relationship between computational cost and number of sectors based on a set of numerical experiments under these conditions. In general, it is suggested that sector length not exceed 1 mile. Naturally, geometric features should be homogeneous within each sector. In addition, the sector length should provide adequate space for the vehicles discharged from the on-ramp during any simulation interval.

TABLE 1 Effect of Section Length (ΔX) on Computational Effort

No. Sectors[a]	ΔX(mile)	CPU[b]	CPU[c]
21	0.3	3.56	9.304
13	0.5	3.25	8.468
7	1.0	2.98	8.042
5	1.5	2.54	6.89
4	2.0	2.01	5.77

Note: In all experiments, $\Delta t = 1$ min, $\Delta m = 10$ vehicles, $V_f = 45$ mph, $V_0 = 6$ mph, $\alpha = \pi$, and simulation period = 60 min.

[a] The last 1 mile of this 7-mile facility was treated as one sector in all the cases reported here.

[b] No intermediate report is included in the program output.

[c] Intermediate report of system performance and all vehicle positions during each simulation interval is included in the output.

Selection of Simulation Time Step Δt

It can generally be expected that a smaller simulation time step Δt will result in greater simulation accuracy, particularly when there are large fluctuations in the vehicle generation pattern or significant variations in traffic conditions from sector to sector. Because traffic performance characteristics are assumed to remain constant during Δt, excessively long simulation intervals will, in general, lead to highly artificial discretized traffic flow. The resulting loss of accuracy is evident in Table 2, which gives a summary of the results of numerical experiments for values of Δt equal to 0.5, 1.0, 1.5, 2.0, and 3.0 min, respectively. For each case, the travel times associated with selected departure times from the same sector are given in this table, indicating that the magnitude of the discrepancies could be substantial, particularly for the largest value of Δt considered here.

TABLE 2 Travel Time (min) Versus Departure Time for Alternative Simulation Time Intervals (Δt), Sector 1

Departure Time (a.m.)	Δt (min)				
	Δt = 0.5	Δt = 1.0	Δt = 1.5	Δt = 2.0	Δt = 3.0
7:15	9.0	9.0	9.0	12.0	18.0
7:20	9.0	9.0	10.0	12.0	18.0
7:25	9.5	10.0	10.5	12.0	18.0
7:30	10.5	11.0	12.0	14.0	30.0
7:35	16.0	17.0	19.5	22.0	36.0
7:40	23.0	22.0	22.5	24.0	39.0
7:45	26.0	25.0	29.0	32.5	36.0

Note: In all cases Δm = 10 vehicles, 400 vehicles/sector, two lanes in each direction, v_f = 45 mph, v_0 = 6 mph, $\alpha = \pi$, and simulation duration = 60 min.

Fortunately, the computational efficiency of this model relieves to a great extent the concern for computation cost in selecting Δt. The computational effort is nonetheless quite sensitive to the size of Δt, as illustrated in the results, given in Table 3, of several numerical experiments.

TABLE 3 Effect of Simulation Time Step (Δt) on Computational Effort

Δt (min)	CPU[a]	CPU[b]
0.5	5.32	14.105
1.0	2.98	8.042
1.5	2.16	5.975
2.0	1.82	4.684
3.0	1.43	3.873

Note: Δm = 10 vehicles/particle, 400 vehicles/sector, two lanes in each sector, v_f = 45 mph, v_0 = 6 mph, $\alpha = \pi$, and simulation duration = 60 min.

[a]No intermediate report is included in the program output.

[b]Intermediate report of system performance and all vehicle positions during each simulation interval is included in the output.

Selection of Macroparticle Size Δm

As described in the previous section, vehicles bound for the same destination are grouped into macroparticles and thus enter the facility simultaneously. Conceptually, no problem would arise if each particle consisted of a variable number of vehicles, which would be specified as an additional attribute identifying each particle. However, for operational convenience, the use of identically sized macroparticles is suggested unless the number of vehicles arriving during Δg is insufficient to meet the prespecified size. In general, heavy traffic generation during the peak period can accommodate any reasonable predetermined particle size.

The specification of the particle size does not appear to significantly affect the accuracy of the simulation, as revealed by several numerical experiments. A summary of the results is given in Table 4, which depicts the travel time associated with various departure times under alternative macroparticle sizes (Δm = 5, 10, 15, and 20 vehicles per particle, respectively). The size of Δm does, however, contribute to the model's computational efficiency, although the marginal contribution of an increase in Δm beyond about 10 vehicles per particle decreases sharply, as seen in Table 5.

TABLE 4 Travel Time (min) Versus Departure Time for Alternative Macroparticle Sizes, Sector 1

Departure Time (a.m.)	Particle Size			
	Δm = 5	Δm = 10	Δm = 15	Δm = 20
7:15	9	9	9	9
7:20	9	9	9	9
7:25	10	10	10	10
7:30	11	11	11	11
7:35	16	17	16	15
7:40	28	26	26	25
7:45	28	29	28	28

Note: In all cases Δt = 1 min, 400 vehicles per sector, two lanes in each direction, v_f = 45 mph, v_0 = 6 mph, $\alpha = \pi$, and simulation duration = 60 min.

TABLE 5 Effect of Macroparticle Size (Δm) on Computational Effort

Δm	CPU[a]	CPU[b]
5	3.541	10.025
10	2.980	8.042
15	2.811	7.854
20	2.703	6.945

Note: In all cases, the following conditions hold: Δt = 1 min, 400 vehicles/sector, two lanes in each direction, v_f = 45 mph, v_0 = 6 mph, $\alpha = \pi$, and simulation duration = 60 min.

[a]No intermediate report is included in the program output.

[b]Intermediate report of system performance and all vehicle positions during each simulation interval is included in the output.

Note that in the selection of Δm, care must be taken to ensure that it is less than the maximum ramp entry rate (per unit simulation time step). A size of 5 vehicles per particle per lane (i.e., 10 vehicles for a facility with two lanes in each direction) has been found particularly convenient and appropriate in these experiments.

In the remainder of this paper an illustration is presented of the application of this model to the type of investigation for which it was developed. In particular, its application to the study of the dynamic behavior of traffic systems during peak-period congestion, under both mathematical decision rules and in conjunction with real commuters supplying departure time information, is described.

APPLICATION 1: SIMULATION EXPERIMENTS TO INVESTIGATE SYSTEM CONVERGENCE

This section contains a description of the use of the MPSM to explore the dynamics of a commuting corridor through a set of simulation experiments aimed at investigating the system's convergence status under alternative behavioral mechanisms. The latter are specified in the user-decisions subroutine introduced in the first section. Note that the presentation herein is intended primarily for illustrative purposes; further discussion of the details of the experiments, of the underlying assumptions, particularly those regarding user behavior, as well as of the results can be found in Mahmassani and Chang (10). In this section, the relevant features of the system and the type of behavioral rules that were considered are presented. Next, the key results per-

taining to system convergence that emerged from this particular set of experiments are highlighted.

System Features and Experimental Conditions

Supply-Side Input

The commuting corridor considered here is comprised of seven 1-mile sectors, with the common single work destination at the end of the seventh (and last) sector, as would be the case for CBD-bound work trips. Sectors are numbered from 1 to 7 in decreasing order of distance from the CBD. The highway facility consists of two lanes in each direction, although only the inbound direction is of concern here, with a mean free speed (v_f) of 40 mph and "jam" concentration (k_0) of 200 vehicles per lane-mile. The maximum entry rate, reflecting physical capacities as well as operational controls, is specified here as a constant of 80 vehicles per minute per sector. Note that a minimum speed of v_0 = 6 mph was specified in all cases to prevent a complete blockage of the system at high concentrations.

Demand-Side Input and User-Decisions Subroutine

The same number of users (in vehicle trips) was assumed for each of Sectors 1 through 6, with no trips generated in Sector 7, which can be viewed as a non-residential fringe sector. For simplicity, and without loss of generality, all commuters in these experiments were assumed to have the same work starting time of 8:00 a.m., although the model allows for a more general distribution of work start times.

Commuter behavior mechanisms of particular interest to this research application were specified in the user-decisions subroutine in order to provide daily departure time distributions. Two basic mechanisms can be distinguished in this subroutine: the first determines the acceptability, to a given user, of his most recent departure time, and the second determines the amount by which an unsatisfied commuter will adjust his departure time on the following day.

The first mechanism reflects a "satisficing," or boundedly rational view of commuter decisions in everyday situations (10,13). Essentially, it states that a user evaluates his departure time choice based on its outcome. A plausible rule is that users will accept a particular departure time, and maintain it on the next day, if the schedule delay, or the discrepancy between the resulting arrival time and the desired arrival time, is less than a certain tolerable level. This "indifference band" of tolerable schedule delay is viewed as a characteristic of each user (j) and is denoted by IB_j. It is natural to expect a distribution of IB_j across the population of commuters; the mean of this distribution, denoted by E[IB], is one of the experimental factors of concern in this research application. Three non-zero values of E[IB] were considered, namely, 5, 10, and 15 min, in addition to the extreme case of no indifference band. The distribution of IB_j across users was taken as a truncated normal distribution, coarsely discretized for the present purpose with a constant variance-to-mean ratio equal to 0.2.

The second mechanism, which specifies the departure time readjustment in response to previous days' performance, has been examined under two possible rules:

- A "myopic" rule, which says that the readjustment depends only on the latest day's schedule delay and
- A "learning" rule, whereby the readjustment explicitly takes into consideration the travel outcomes on more than just the latest day; typically, the relative weight accorded to recent experience is greater than that accorded to earlier experience.

The specific mathematical expressions for these mechanisms are presented in the Appendix. Simulation experiments were conducted to explore the dynamics of the system's behavior under the alternative myopic or learning readjustment rules. In addition, these experiments addressed the effect of two key factors: (a) the mean indifference band (E[IB]) for which the four different cases mentioned earlier were considered and (b) the usage level, whereby three different values were considered: a "reference" value V = 420 vehicles per sector, and V_1 = 0.6V and V_2 = 1.4V. The interaction between the usage level and the indifference band in determining the system's convergence properties is of particular interest and is described hereafter. Note that other factors, such as the parameters of the previously mentioned mechanisms (see Appendix) and the system's initial conditions (specified in terms of initial departure time distribution for each sector), were also explored, as described elsewhere (10).

Summary of Results

The corridor system was simulated for a period ranging from 50 to 70 consecutive days under each combination of values for the mean indifference band and the usage level, for both myopic and learning departure time adjustment rules. Convergence is examined in terms of the departure time distribution in each sector. When all users in a sector settle on their respective departure times, steady state is attained in that sector. For each simulation, the state of each sector after 70 days was recorded as one of the following: C for convergence to a steady state, O for regular oscillatory behavior, or NC for no convergence. A summary of this information is given in Table 6 for all the experiments in which the myopic adjustment rule was used and in Table 7 for those in which the learning-based rule was used. In both tables the number of days after which a steady state or regular oscillations were attained is indicated (in parentheses following the symbols C or O, respectively), where applicable. Note that in those situations where steady state or regular oscillations were not attained in all six sectors, partial steady state or oscillations, or both in only some of the sectors, are not necessarily guaranteed to be maintained indefinitely (10).

Effect of Mean Tolerable Schedule Delay

The data in both Tables 6 and 7 reveal that, all else being equal, the system is more likely to stabilize for larger values of E[IB]. This seems to be the case under both myopic and learning-based adjustment rules. For instance, consider the state of the system under experiments 2, 5, 8, and 11 in Table 7, corresponding to E[IB] values of 0, 5, 10, and 15 min, respectively. For the largest E[IB] value of 15 min, convergence to a steady state is reached in all sectors by Day 13. For E[IB] = 10 min, only partial convergence is attained, with the three sectors closest to the destination attaining a steady state, and under E[IB] = 5 min, convergence occurs in Sectors 5 and 6 only. Finally, under the assumption of no tolerable schedule delay, only sector 6 attains a steady state. This suggests the existence of a critical, or threshold, level of tolerable schedule delay above which a given system will be able to reach a steady state. This critical

TABLE 6 State of System After 70 Days, Myopic Behavior

Experiment No.	Usage Level[a]	Sector 1	2	3	4	5	6
No Indifference Band; E[IB] = 0							
1	0.6V	NC	NC	NC	NC	NC	C(14)
2	V	NC	NC	NC	NC	NC	C(37)
3	1.4V	NC	NC	NC	NC	NC	NC
Mean Tolerable Schedule Delay E[IB] = 15 Min							
4	0.6V	NC	NC	NC	NC	C(50)	C(56)
5	V	NC	NC	NC	NC	C(64)	C(12)
6	1.4V	NC	NC	NC	NC	NC	NC
E[IB] = 10 Min							
7	0.6V	C(8)	C(8)	C(18)	C(7)	C(8)	C(7)
8	V	O(46)	O(46)	C(45)	C(34)	C(7)	C(7)
9	1.4V	NC	NC	NC	NC	C(44)	C(10)
E[IB] = 15 Min							
10	0.6V	C(7)	C(7)	C(7)	C(7)	C(7)	C(7)
11	V	C(14)	C(13)	C(14)	C(13)	C(8)	C(4)
12	1.4V	NC	NC	NC	NC	C(9)	C(9)

Note: NC = no convergence by Day 70; C(I) = convergence achieved after I days; O(I) = regular oscillations started after I days.

[a]V is the reference value of 420 vehicles per sector.

TABLE 7 State of System After 70 Simulation Days, Learning Behavior

Experiment No.	Usage Level[a]	Sector 1	2	3	4	5	6
No Indifference Band; E[IB] = 0							
1	0.6V	NC	NC	NC	NC	NC	C(32)
2	V	NC	NC	NC	NC	NC	C(55)
3	1.4V	NC	NC	NC	NC	NC	NC
Mean Tolerable Schedule Delay E[IB] = 5 Min							
4	0.6V	NC	NC	NC	NC	C(8)	C(4)
5	V	NC	NC	NC	NC	C(36)	C(6)
6	1.4V	NC	NC	NC	NC	NC	NC
E[IB] = 10 Min							
7	0.6V	C(9)	C(10)	C(10)	C(9)	C(9)	C(4)
8	V	NC	NC	NC	C(52)	C(6)	C(6)
9	1.4V	NC	NC	NC	NC	C(48)	C(9)
E[IB] = 15 Min							
10	0.6V	C(6)	C(6)	C(7)	C(5)	C(6)	C(4)
11	V	C(11)	C(12)	C(11)	C(12)	C(13)	C(4)
12	1.4V	NC	NC	NC	NC	C(21)	C(9)

Note: NC = no convergence by Day 70; C(I) = convergence achieved after I days; O(I) = regular oscillations started after I days.

[a]V is the reference of 420 vehicles per sector.

level would essentially reflect the users' flexibility and willingness to compromise. The tighter this tolerable amount, the less likely it is that users will be able to reach a stable state (or a repeatable daily routine). It can also be noted that, all else being equal, the time needed to reach a steady state in a given sector appears to increase as the tolerable schedule delay increases.

Effect of Usage Level

The data in Tables 6 and 7 also reveal that, for a given E[IB], the system is more likely to converge at lower than at higher demand levels. Furthermore, higher usage levels (number of trip makers per sector) require a longer period to converge. For instance, consider experiments 10, 11, and 12 in Table 7, corresponding to usage levels of 0.6V (V = 420 vehicles per sector) and 1.4V, respectively, with E[IB] = 15 min. At the highest demand of 1.4V, only the last two sectors appear to have reached a steady state. At the reference demand level V, all sectors converge to a steady state as of Day 13. On the other hand, at the lowest usage level considered, 0.6V, convergence to steady state is reached in all sectors as of Day 7. The same general effect of the usage level can be observed in all the other experiments summarized in Tables 6 and 7.

In summary, there appears to be a strong inter-

relation between the usage level and the amount of tolerable schedule delay in determining the ability of the system to converge to a steady state, as well as the duration needed to achieve this convergence. Heavy traffic levels require wider indifference bands on behalf of system users, reflecting greater tolerance for delay, for a given system to equilibrate. It can also be noted that sectors closer to the destination generally attain their steady state sooner than more distant sectors and at lower values of E[IB] for a given usage level. This implies that more distant trip makers must be prepared to tolerate greater delay for the system to equilibrate, which is important in the design and evaluation of demand-side congestion relief measures.

APPLICATION 2: INTEGRATION OF SURVEY TECHNIQUES AND COMPUTER SIMULATION

Instead of employing prespecified mathematical expressions to supply users' decisions in the simulations, a number of real commuters were asked to take part in an experiment in which they provided daily departure time choices in a given hypothetical situation. Detailed description and in-depth analysis of the experimental results can be found elsewhere (4). A summary of this research and highlights of its results, with emphasis on congestion dynamics and system convergence, are presented in this section.

Description of Experiment

Much like the example application described in the previous section, the commuting corridor considered here consists of a highway facility used by adjoining residents for their daily home-to-work commute to a single work destination (CBD). This facility of two lanes in each direction is subdivided into nine identical 1-mile sectors, with the common work destination at the end of the last sector. Sectors are numbered from 1 through 9, with Sector 1 being the farthest outbound and Sector 9 the closest to the destination. The parameters used in the MPSM were v_f = 40 mph, v_0 = 6 mph, k_0 = 180 vehicles per lane-mile, and the maximum entry rate is taken as a constant equal to 60 vehicles per minute.

A total of 400 trip makers was assumed in each of the five residential sectors (from Sector 1 through Sector 5). A total of 100 participants was involved in this experiment, with each participant in effect representing 20 vehicles (or one macroparticle in each lane, with m = 10) in the MPSM program.

Each participant was initially given information about the highway facility (free speed, number of lanes) and his location, as well as the familiar decision situation of starting work at 8:00 a.m. Under those conditions participants were asked to state their desired arrival time and the corresponding departure time. The departure time decisions of all participants were obtained daily and input into the MPSM. The latest outcome of their choices, namely the respective actual arrival time on the previous day, as determined by the simulation, was provided to each participant individually on the following day, before his choice for that day was made. To relate the experiment to participants' actual daily commute, the survey was administered 5 days per week during the entire survey period.

Note that, because departure times were determined directly by actual commuters, there was no need to specify a user-decisions subroutine in this case.

SUMMARY OF EXPERIMENTAL RESULTS

System Convergence

This experiment covered 24 days, at which time all sectors in the system had already attained a steady state. The day-to-day evolution of average travel time over the period of the experiment is shown in Figure 3. It can be seen that the system's performance did not change as of Day 21. The steady-state values were actually attained on Day 18, exhibiting a fluctuation on Day 20 due to a few participants' (in Sector 1) unsuccessful attempt to improve their outcome, after which they reverted back to their steady-state choices (see Figure 4).

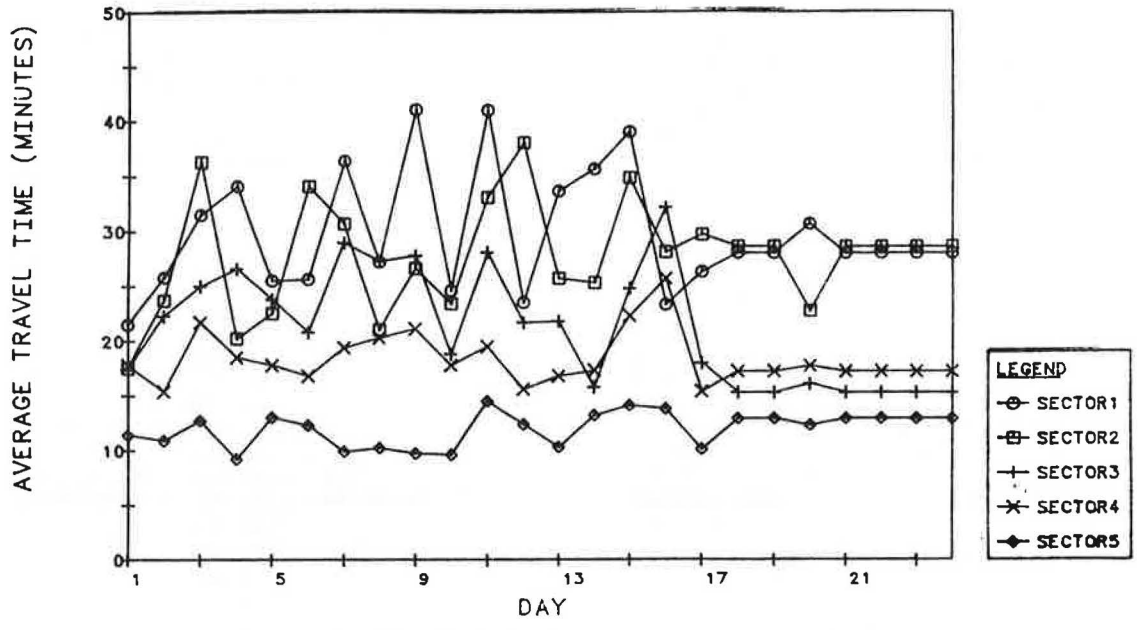

FIGURE 3 Evolution of average travel time for each sector.

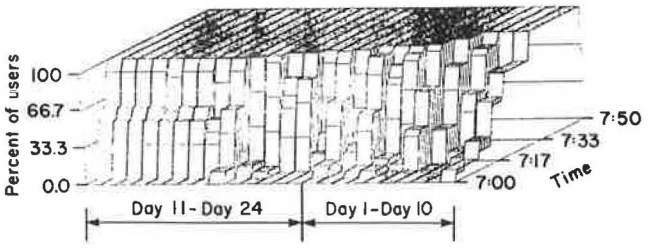

FIGURE 4 Cumulative departure pattern evolution for Sector 1.

An examination of the day-to-day evolution of the cumulative departure time distributions in each sector, considered separately, reveals that sectors with less travel distance tend to reach their steady-state values earlier than more distant sectors. This is exemplified by the day-to-day patterns for Sectors 1 and 5, respectively the farthest and closest, as shown in Figures 4 and 5. It can be seen in Figure 5 that all users in Sector 5 maintained their departure time choices as of Day 5, whereas Figure 4 indicates that the steady-state distribution in Sector 1 was completely reached as of Day 21. This phenomenon is consistent with the conclusions suggested by the simulation experiments described in the previous section.

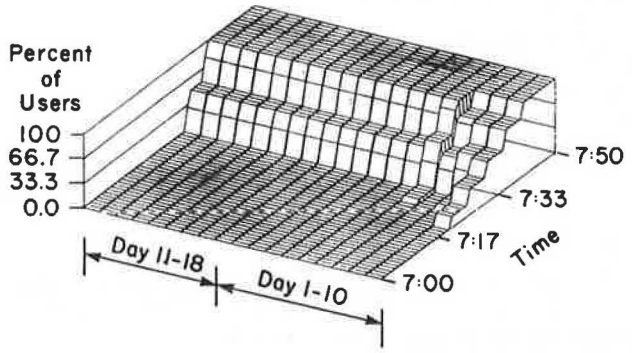

FIGURE 5 Cumulative departure pattern evolution for Sector 5.

The day-to-day variation of the average schedule delay of users in each sector is shown in Figure 6. It is worth noting that the average schedule delay, observed at steady state, increases in magnitude with increasing travel distance. In other words, commuters located in distant sectors have to tolerate longer schedule delays than those in near sectors in order to converge to a steady state. This interesting result is consistent with the conclusion of the simulation experiments described in the previous section.

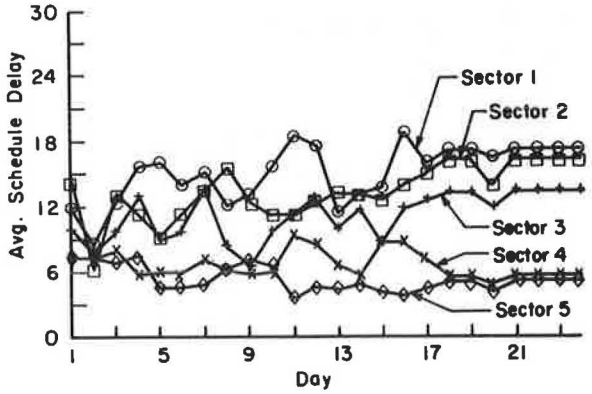

FIGURE 6 Evolution of average schedule delay for each sector.

Congestion Evolution and Travel Time Variability

The time-dependent pattern of traffic concentration in each sector is shown in Figures 7-11 for each of the first 5 days (first week), respectively. It can be seen that congestion was not severe on Day 1, with concentration in most sectors remaining below $2k_0/3$ (120 vehicles per lane-mile). A general worsening on Days 2 and 3 can be detected, with Sectors 3 through 5 and Sectors 7 through 9 manifesting

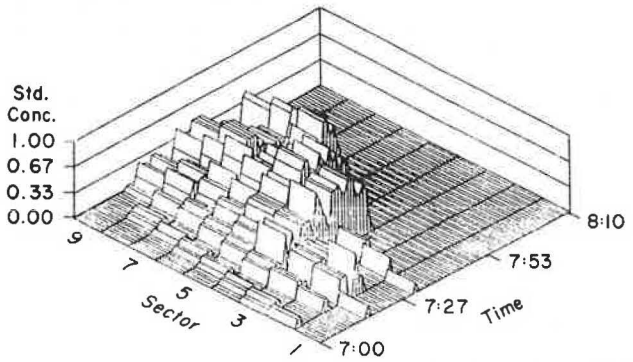

FIGURE 7 Time-dependent concentration pattern on Day 1, by sector.

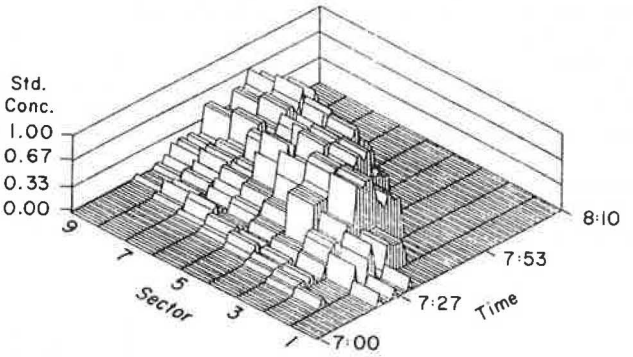

FIGURE 8 Time-dependent concentration pattern on Day 2, by sector.

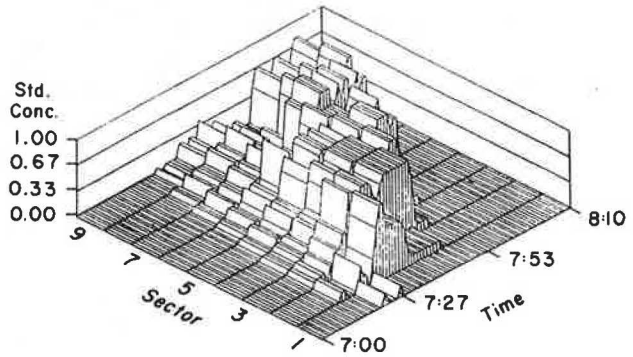

FIGURE 9 Time-dependent concentration pattern on Day 3, by sector.

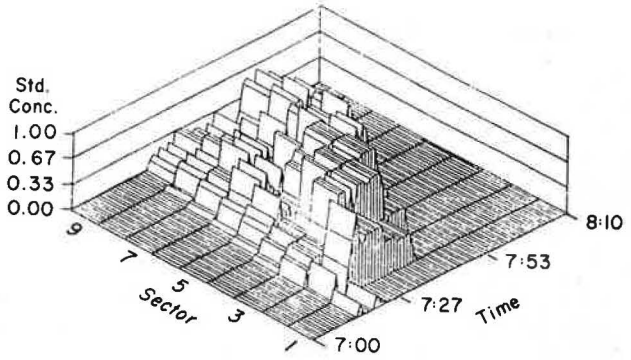

FIGURE 10 Time-dependent concentration pattern on Day 4, by sector.

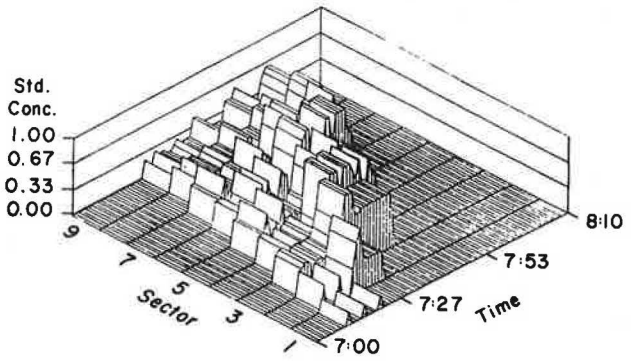

FIGURE 11 Time-dependent concentration pattern on Day 5, by sector.

relatively long periods of high concentration. Users' responses to these high levels led to a shift of the concentration distribution on Day 4 to an earlier time relative to Day 3 in all sectors; the overall pattern on Day 4 is quite similar to that of Day 2. Conversely, the temporal distributions of the concentration in all sectors moved forward on Day 5, resulting in a pattern that is similar to that of Day 3, except that the magnitude of the shift was less drastic on Day 5 than on Day 3. In other words, the range of the day-to-day fluctuation of concentration appeared to be narrowing until steady state was reached. This phenomenon can be attributed to the effect of commuters' previous experience with their departure time choices. Detailed discussion regarding commuters' departure time choice behavior and its interaction with congestion variation is outside the scope of the present paper and can be found elsewhere (10,14).

The steady-state time-dependent concentration pattern in each sector is shown in Figure 12, which reveals the high congestion periods for each sector. In addition, a typical example of the day-to-day evolution of the time-dependent concentration is shown in Figure 13 for Sector 3.

Table 8 gives a further summary of congestion patterns; of concern are both the occurrence of high concentration periods and their duration. Operationally, and somewhat arbitrarily, high congestion in a given sector was defined as the occurrence of 3 or more minutes within which concentration was continuously greater than or equal to $2k_0/3$. The duration of periods in which this criterion held, in each sector, is given on a daily basis in Table 8. Apparently, Sectors 3 through 5 experience the longest high congestion periods at steady state as well as

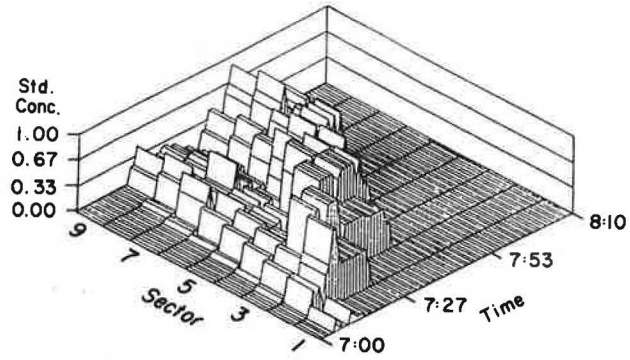

FIGURE 12 Time-dependent concentration pattern at steady state, by sector.

throughout the duration of the experiment. This congestion, with a time lag, spreads to downstream sectors, which experience shorter congestion periods overall.

The record of travel time fluctuation for different departure times in each sector is one of the principal results of the MPSM. The steady-state pattern of travel time versus departure time [Figure 14 (d)] exhibits clear peaking characteristics with more distant sectors experiencing higher peaks than closer sectors. The peaking phenomenon, initially not very pronounced on Day 1 [Figure 14(a)], becomes more distinct as the system evolves, as illustrated by the patterns for Days 1, 6, and 11, and at steady state [Figure 14(a), (b), (c), and (d), respectively].

The extent of the sensitivity of travel time to the choice of departure time can also be seen from these patterns. For instance, if a commuter were to depart (at steady state) from Sector 1 at 7:10 a.m. instead of 7:05 a.m., he would experience as much as a 30-min increase in travel time. Similar situations also exist in other sectors, although sensitivity to departure time choice is somewhat less drastic in closer sectors.

TABLE 8 High Congestion Duration in Each Sector[a] (min)

	Sector								
Day	1	2	3	4	5	6	7	8	9
1	0	0	0	22	23	8	0	4	0
2	0	0	14	23	23	11	7	0	0
3	0	0	21	20	24	13	17	7	4
4	0	10	15	17	18	11	3	3	0
5	0	0	16	15	9	21	15	8	4
6	0	13	16	16	22	7	7	7	4
7	0	19	21	20	26	7	17	10	6
8	0	0	20	25	21	3	0	0	0
9	0	21	25	26	24	6	4	5	0
10	0	0	19	13	12	3	6	0	0
11	0	14	27	27	27	22	20	0	0
12	0	13	16	17	15	17	4	0	0
13	0	14	17	20	19	11	8	3	0
14	0	12	8	14	13	16	7	3	0
15	0	11	25	25	28	7	4	6	4
16	0	0	14	22	24	16	7	5	0
17	0	7	8	19	15	10	7	8	4
18	0	5	22	17	17	16	10	7	5
19	0	4	22	17	17	8	7	10	5
20	0	13	19	18	14	8	15	7	3
21[b]	0	4	22	17	17	8	7	10	5

[a]High congestion is defined as the occurrence of $k \geq 2k_0/3$ for more than 3 min.
[b]Days 22-24 are identical to Day 21.

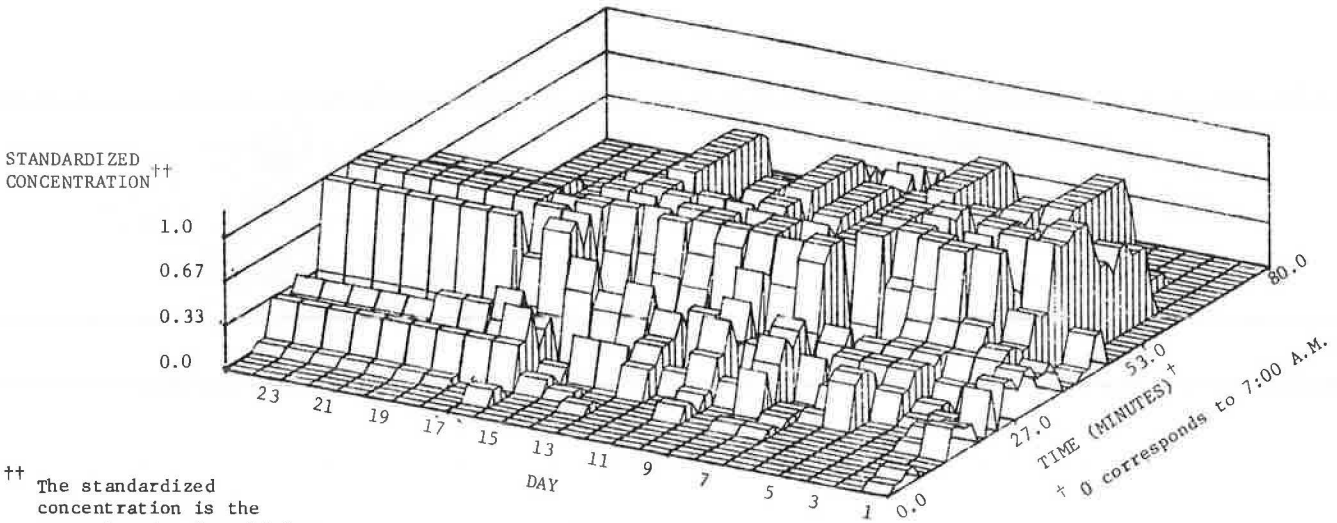

†† The standardized concentration is the concentration in vehicles per lane-mile normalized by the "jam" concentration.

FIGURE 13 Evolution of time-dependent concentration pattern, Sector 3.

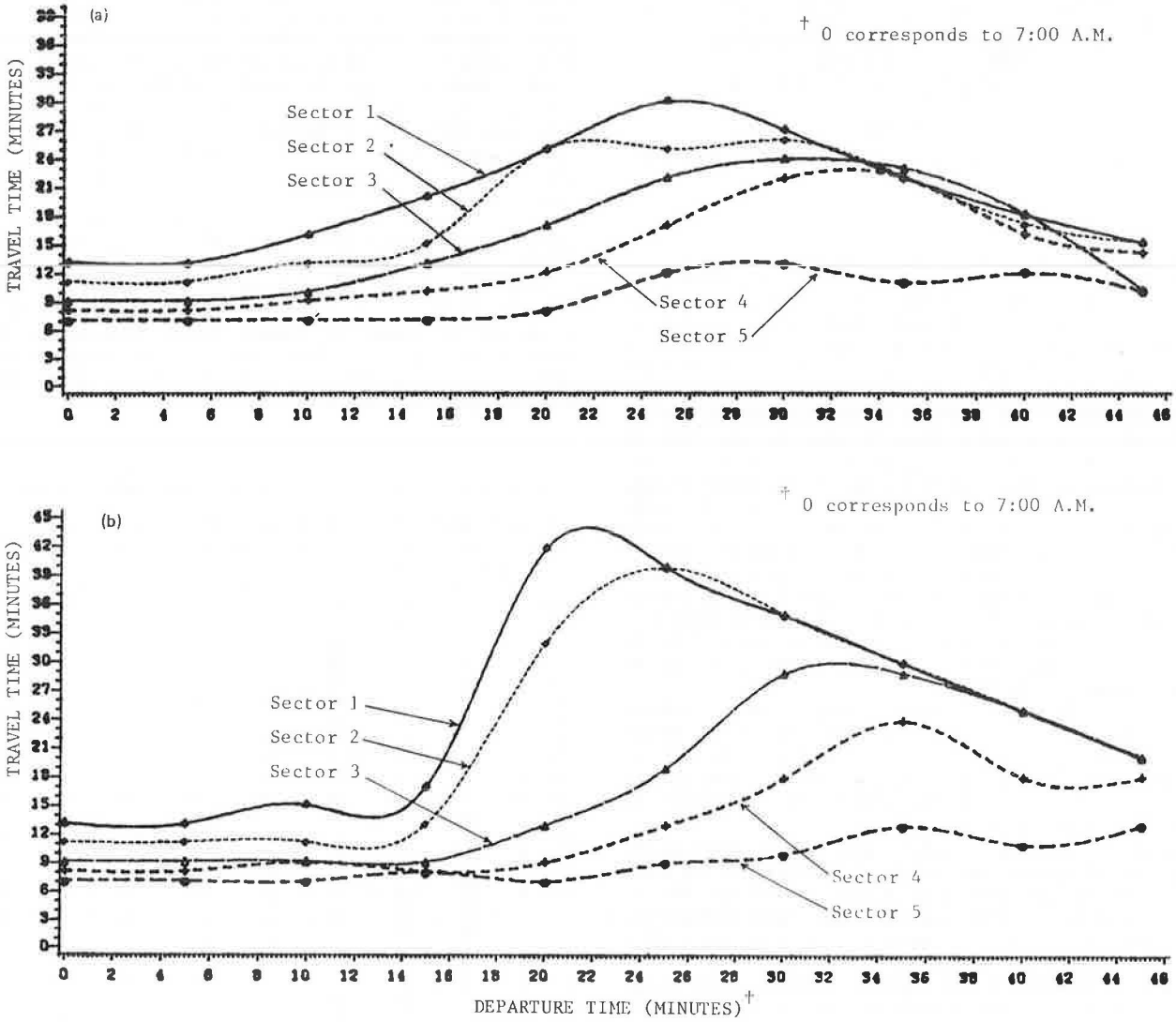

FIGURE 14 Travel time versus departure time on selected days, by sector: (a) Day 1; (b) Day 6; (c) Day 11; (d) Day 24, steady state.

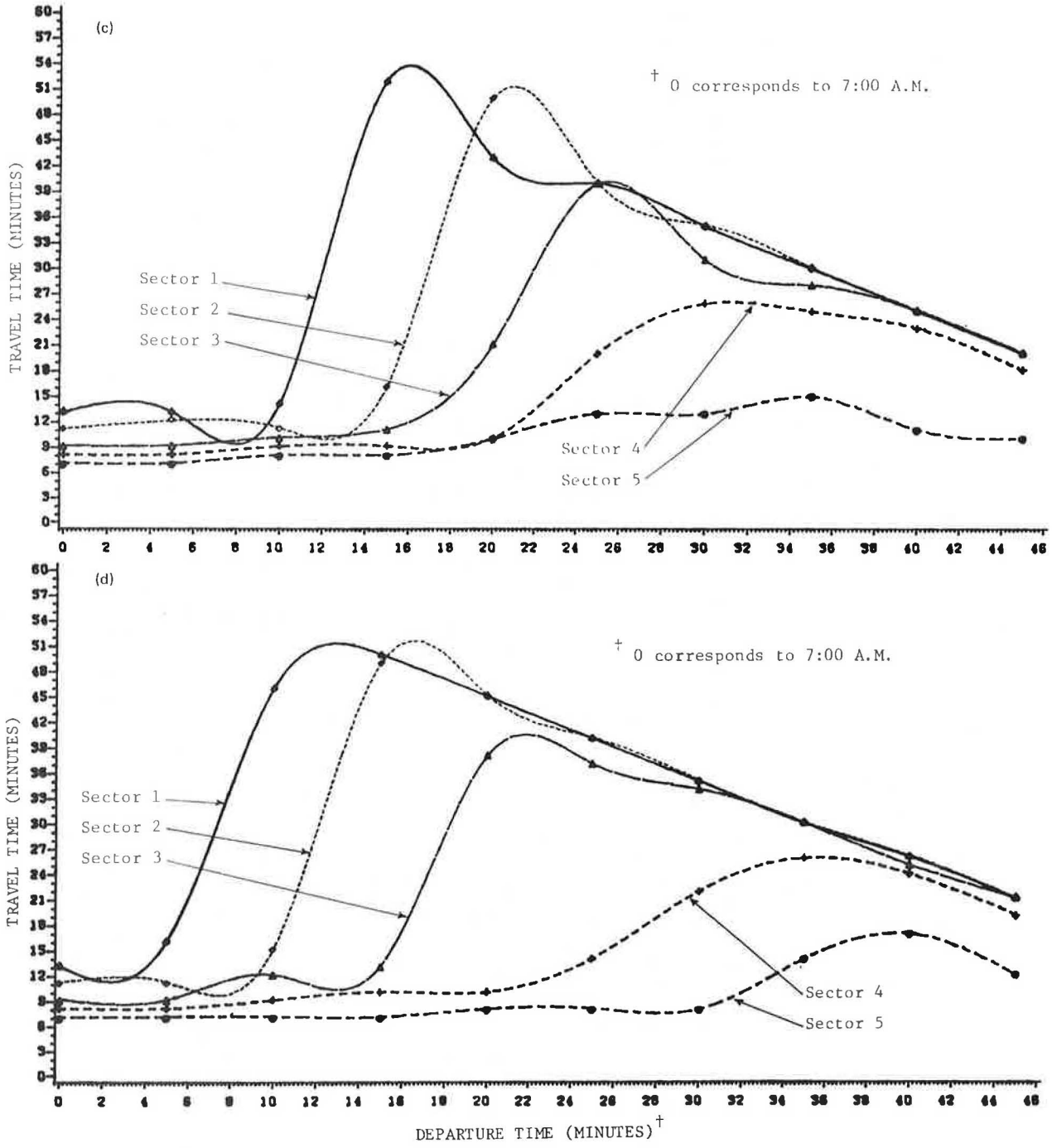

FIGURE 14 continued.

CONCLUSION

A special-purpose macroscopic model for the simulation of highway corridor traffic has been presented. The model was developed in conjunction with studies of the dynamics of peak-period traffic congestion in commuting systems and the interrelation between user decisions and congestion formation and dissipation. The model moves vehicles in small bunches or macroparticles using local speeds defined by the speed-concentration relation resulting in high computational efficiency, which is essential for the type of application for which the model is intended.

The details of merging and passing maneuvers are not captured by the simulation. However, the simulated system's behavior has been found adequate to pursue the investigation of peak-period congestion dynamics. Two such applications of the model have been presented: In the first, users' daily departure time decisions were simulated by the model using a set of specified dynamic decision rules. In the other application, a number of real commuters participated in a novel interactive experiment in which the traffic simulation model was used to determine each participant's arrival time, given all participants' departure time decisions for that day.

To further support this investigation of the dynamics of peak-period congestion, the following extensions and modifications of the MPSM are under way: (a) inclusion of more than one route, whereby

users can select both their departure time and their route; (b) better representation of traffic control devices, particularly at the entry points, to enhance the model's capability to evaluate traffic-based congestion relief measures; and (c) incorporation of the commuter's search for a parking space at the work destination, which is of particular relevance for downtown-oriented commuting in many large cities.

ACKNOWLEDGMENTS

The work reported herein was partly funded by a grant (to H. Mahmassani) from the Bureau of Engineering Research at the University of Texas at Austin. Computer funds made available by the Department of Civil Engineering, the Center for Studies in Statistical Mechanics, and the Physics Department at the university are gratefully acknowledged. Initial work on the development of the traffic simulation model was performed by Sonia Claudet, formerly a research scientist in the Center for Studies in Statistical Mechanics. In addition, the authors would like to thank T. Tajima, Department of Physics at the University of Texas at Austin, for alerting them to his work on the magnetohydrodynamic particle code for the simulation of plasmas. Finally, the assistance of Alfredo Hinojos in the preparation of the graphic material is appreciated. Support for the revision and continuation of this research is provided by NSF Grant CEE-8400306.

REFERENCES

1. C. Hendrickson and G. Kocur. Schedule Delay and Departure Time Decisions in a Deterministic Model. Transportation Science, Vol. 15, No. 1, 1981, pp. 62-77.
2. C. Hendrickson, D. Nagin, and E. Plank. Characteristics of Travel Time and Dynamic User Equilibrium for Travel-to-Work. In Proceedings of the Eighth International Symposium on Transportation and Traffic Theory, V.F. Hurdle, E. Hauer, and G.N. Steuart, eds., University of Toronto Press, Canada, 1983, pp. 321-347.
3. P.H. Fargier. Effects of the Choice of Departure Time on Road Traffic Congestion: Theoretical Approach. In Proceedings of the Eighth International Symposium on Transportation and Traffic Theory, V.F. Hurdle, E. Hauer, and G.N. Steuart, eds., University of Toronto Press, Canada, 1983, pp. 223-263.
4. A. De Palma, M. Ben-Akiva, C. Lefevre, and N. Litinas. Stochastic Equilibrium Model of Peak Period Traffic Congestion. Transportation Science, Vol. 17, No. 4, 1983, pp. 430-453.
5. H. Mahmassani and R. Herman. Dynamic User Equilibrium Departure Time and Route Choice on Idealized Traffic Arterials. Transportation Science, Vol. 18, No. 4, 1984, pp. 362-384.
6. D.N. Goodwin, S.D. Miller, and H.J. Payne. MACK: A Macroscopic Simulation Model of Freeway Traffic. Technology Service Corp., Santa Monica, Calif., 1974.
7. H.J. Payne. FREFLO: A Macroscopic Simulation Model of Freeway Traffic. In Transportation Research Record 722, TRB, National Research Council, Washington, D.C., 1979, pp. 68-75.
8. E.B. Lieberman. Dynamic Analysis of Freeway Corrdior Traffic. Presented at the Joint Transportation Engineering Conference, American Society of Mechanical Engineers, Chicago, Ill., 1970.
9. E.B. Lieberman. Simulation of Corridor Traffic: The SCOT Model. In Highway Research Record 409, HRB, National Research Council, Washington, D.C., 1972, pp. 34-45.
10. H.S. Mahmassani and G.-L. Chang. Experiments with Departure Time Choice Dynamics of Urban Commuters. Transportation Research B (in press).
11. A.D. May. Models for Freeway Corridor Analysis. In TRB Special Report 194: The Application of Traffic Simulation Models, TRB, National Research Council, Washington, D.C., 1981, pp. 23-32.
12. N.A. Derzko, A.J. Ugge, and E.R. Case. Evaluation of a Dynamic Freeway Flow Model Using Field Data. Presented at 62nd Annual Meeting of the Transportation Research Board, Washington, D.C., 1983.
13. J.N. Leboeuf, T. Tajima, and J.M. Dawson. A Magnetohydrodynamic Particle Code for Fluid Simulation of Plasmas. Journal of Computational Physics, Vol. 31, No. 3, June 1979, pp. 379-408.
14. H.S. Mahmassani, G.-L. Chang, and R. Herman. Individual Decisions and Collective Effects in a Simulated Traffic System. Transportation Science (in press).

APPENDIX: EQUATIONS FOR USER-DECISIONS SUBROUTINE

Two basic equations govern the dynamics of user departure time decisions in the commuting corridor. The first equation simply determines acceptability of a given departure time on the basis of its outcome. Let $D_{j,t}$ and $AT_{j,t}$ denote user j's departure time and the resulting actual arrival time at work, respectively, on day t. The mechanism for the acceptability of this outcome used in the simulation experiments, and based on the notation of indifference band, states that

$$\delta_{j,t} = \begin{cases} 1 & \text{if } |AT_{j,t} - DAT_j| \leq IB_j \\ 0 & \text{otherwise} \end{cases}$$

where $\delta_{j,t}$ is a binary variable that takes the value 1 if the actual arrival time on day t is acceptable to user j and 0 otherwise, DAT_j is the desired arrival time of user j, and IB_j is the indifference band, or tolerable schedule delay, of user i. Note that different indifference bands could be specified for earliness as opposed to lateness (10); however, this distinction was not made in the experiments reported in this paper, for the sake of simplicity. Furthermore, IB_j could be specified as varying from day to day, though it was treated as constant, for a given individual in these experiments, for lack of a clear explanatory mechanism for this daily variation. This aspect is the subject of ongoing research by the authors.

The second equation governing user behavior is the departure time readjustment whereby $D_{j,t+1}$ is determined given that $\delta_{i,t} = 1$. Two alternative rules were described in the third section: a myopic rule and a learning-based rule. In both cases, the commuter can be viewed as setting $D_{j,t+1}$ by subtracting his anticipated travel time $ATT_{j,t+1}$, on day t+1, from his desired arrival time, as follows:

$$D_{j,t+1} = DAT_j - ATT_{j,t+1}$$

The myopic and learning rules differ in how $ATT_{j,t+1}$ is obtained given user j's prior experience.

Rule 1: Myopic Adjustment

$$ATT_{j,t+1} = TT_{j,t} + a\gamma^{e}_{j,t}(AT_{j,t} - DAT_j) + b\gamma^{\ell}_{j,t}(AT_{j,t} - DAT_j)$$

where

$TT_{j,t}$ = actual trip time experienced by user j on day t;
$\gamma^{e}_{j,t}$ = a binary variable equal to -1 if $(AT_{j,t} - DAT_j) < 0$ (i.e., user j is early on day t) and 0 otherwise;
$\gamma^{\ell}_{j,t}$ = a binary variable equal to -1 if $(AT_{j,t} - DAT_j) > 0$ (i.e., user j is late on day t) and 0 otherwise, and
a,b = two parameters in the interval [0,1].

The values a = 0.5, b = 0 were used in the experiments described in the third section of this paper. Sensitivity analysis with respect to these parameters as well as an in depth discussion of the embedded behavioral assumptions can be found elsewhere (10).

Rule 2: Learning-Based Adjustment

Here $ATT_{j,t+1}$ is a function of all prior experience with the system, as follows:

$$ATT_{j,t+1} = \sum_{\ell=t_o}^{t} w_\ell \, (TT_{j,\ell})$$

where, w_ℓ, $\ell = t_o,\ldots,t$ denotes a set of non-negative weights attached to each day, starting with the initial day t_o. It is expected that users attach greater weight to more recent days than to earlier ones. Therefore, the following special form of the equation was used in the experiments:

$$ATT_{j,t+1} = [(1 - w_t)/(t - t_o)] \left(\sum_{\ell=t_o}^{t} TT_{j,\ell} \right) + w_t \, TT_{j,t}$$

where $0 < w_t \leq 1$. Thus all days before the last one are given a total weight of $(1 - w_t)$, equally allocated among all prior days; the last day is given a weight w_t. In the experiments reported in the third section of this paper, a value of 0.5 was used for w_t. The effect of the value of this parameter on system behavior does not, however, affect the general conclusions of the third section, as shown elsewhere (10).

Publication of this paper sponsored by Committee on Traffic Flow Theory and Characteristics.

Creation of Data Sets To Study Microscopic Traffic Flow in Freeway Bottleneck Sections

STEVEN A. SMITH and MARK E. ROSKIN

ABSTRACT

The methodologies employed in an FHWA research study entitled "Freeway Data Collection for Studying Vehicle Interactions" are described. The purpose of this study was to develop a series of data sets on microscopic vehicular traffic flow for selected types of freeway sections. The methodology used to develop these data sets involved digitizing vehicle positions from time-lapse aerial photographs of a series of freeway sites with various geometric configurations. Six types of freeway geometry were of interest: ramp merges, weaving sections, upgrade sections, reduced-width sections, lane drops, and horizontal curves. The aerial photography involved the use of a full-frame 35-mm motion picture camera operating in time-lapse mode mounted in a fixed-wing, short-takeoff-and-landing (STOL) aircraft. The sites were filmed at one frame per second with the aircraft flying clockwise at a slow speed around each site at altitudes ranging between 2,500 and 4,500 ft. Data were reduced to 1 hour of film (3,600 frames) of each site. Sites ranged between 1,200 and 3,200 ft in length. The data reduction method involved a microcomputer-based digitizing system. The most important components of the system were the mathematical techniques for computing vehicle position and the method of vehicle matching, which yielded complete vehicle trajectories for all vehicles passing through the sections studied. The data sets are expected to be useful both for empirical research on freeway traffic flow and for the validation of freeway simulation models. The data sets are being made available to those conducting research in these areas.